9-Pyrrolidinylfluorene: colorless needles (MeOH), mp 93 °C; ^{1}H NMR δ 7.5 (m, 8 H), 5.1 (s, 1 H), 2.7 (t, 4 H), 1.7 (m, 4 H). Anal. Calcd for $C_{17}H_{17}N$: C, 86.77; H, 7.29. Found: C, 87.02; H, 7.34.

9-Piperidinylfluorene: colorless needles (MeOH), mp 89 °C; ^{1}H NMR δ 1.43 (br m, 6 H), 2.5 (br t, 4 H), 5.72 (s, 1 H), 7.2–7.7 (m, 8 H).

9-(Diethylamino)fluorene: Bright yellow oil, bp 138–140 °C (1 mm); ^{1}H NMR δ 1.1–0.9 (t, 6 H), 2.7–2.4 (q, 4 H), 4.81 (s, 1 H) 7.65–7.05 (m, 8 H); MS, *m/e* 237 (M^+, 8.3), 222 (8.7), 166 (14.9), 165 (100).

9-(2,6-Dimethylpiperidinyl)fluorene: mp 83.5–84.5 °C; ^{1}H NMR δ 7.1–7.8 (m, 8 H), 5.2 (5, 1 H), 3.1 (m, 1 H), 1.3–1.8 (m, 6 H), 0.6–0.8 (d, 6 H); MS, *m/e* 277 (2.2), 262 (12.9), 166 (22.1), 165 (100).

9-Imidazolylfluorene: mp 151–151.5 °C; ^{1}H NMR δ 7.2–7.7 (m, 9 H), 7.0 (s, 1 H), 6.6 (s, 1 H), 6.0 (s, 1 H); MS, *m/e* 232 (19.5), 166 (14.5), 165 (100.0). Anal. Calcd for $C_{16}H_{12}N_2$: C, 82.73; H, 5.22; N, 12.07. Found: C, 82.92; H, 5.22; N, 12.08.

2,7-Dimethoxy-9-pyrrolidinylfluorene. 2,7-Dimethoxyfluorenone (0.36 g, 1.5 mmol) was dissolved in 5 mL of methanol and reduced with $NaBH_4$ (0.084 g, 2 mmol). The crude alcohol obtained as a colorless solid on workup was suspended in benzene and treated with 0.6 mL of acetyl bromide in 5 mL of acetonitrile. After 1 h at 45 °C the solvent was removed and the solid was washed with water and crystallized from EtOH. The bromide (0.15 g, yellow crystals) was refluxed in 1.5 mL of pyrrolidine for 1 h. After quenching with water, extraction with ether and evaporation of the solvent yielded colorless needles: mp 122.5–123 °C (EtOH); ^{1}H NMR δ 1.78 (m, 4 H), 2.76 (m, 4 H), 3.91 (s, 6 H), 6.96 (dd, 2 H), 7.25 (d, 2 H), 7.57 (d, 2 H).

Electrochemistry. The measurements of cyclic voltammograms were carried out as previously described.[25]

Acknowledgment is made to the donors of the Petroleum Research Fund, administered by the American Chemical Society, and to the National Science Foundation for support of this work. We thank Dr. A. V. Satish for the preparation of 2,7-bis(dimethylamino)fluorene and for the acidity and oxidation potential measurements made with this compound.

Registry No. $PhCH_2Cl$, 100-44-7; 9-Me_2NFl^-, 83936-70-3; 9-piperidinyl-Fl^-, 111933-72-3; 9-pyrrolidinyl-Fl^-, 111933-71-2; 9-azetidinyl-Fl^-, 111933-70-1; 9-Et_2NFl^-, 116997-61-6; 9-(2-methylpiperidinyl)Fl^-, 111933-73-4; 9-*t*-Pr_2NFl^-, 109495-02-5; 9-(2,2,6,6-tetramethylpiperidinyl)Fl^-, 111933-74-5; 9-(3-methyl-1-pyrazolyl)Fl^-, 116997-62-7; 9-(1-imidazolyl)Fl^-, 116997-63-8; FlH_2, 86-73-7; 2-$MeOFlH_2$, 2523-46-8; 2,7-$(MeO)_2FlH_2$, 42523-30-8; 2-Me_2NFlH_2, 13261-62-6; 2,7-$(Me_2N)_2FlH_2$, 13261-63-7; 9-Me_2NFlH, 53156-46-0; 9-Et_2NFlH, 108975-83-3; 9-*i*-Pr_2NFlH, 109495-00-3; 9-azetidinyl-FlH, 116997-64-9; 9-pyrrolidinyl-FlH, 7596-59-0; 2,7-$(MeO)_2$-9-pyrrolidinyl-FlH, 116997-65-0; 9-piperidinyl-FlH, 3333-06-0; 9-(2,6-piperidinyl)-FlH, 116997-66-1; 9-imidazolyl-FlH, 35214-35-8; 2,7-$(MeO)_2$-9-imidazolyl-FlH, 116997-67-2; 9-*n*-BuNHFlH, 46880-06-2; 9-$Me_3NFlH^+Br^-$, 6634-60-2; FlH^-, 12257-35-1; 2-$MeOFlH^-$, 100858-88-6; 2,7-$(MeO_2)FlH^-$, 100858-87-5; 2-Me_2NFlH^-, 113533-33-8; 2,7-$(Me_2N)FlH^-$, 116997-68-3; 2,7-$(MeO)_2$-9-pyrrolidinyl-Fl^-, 116997-69-4; 9-(2,6-dimethylpiperidinyl)-Fl^-, 116997-70-7; 2,7-$(MeO)_2$-9-imidazolyl-Fl^-, 116997-71-8; 9-*n*-$BuFl^-$, 116997-72-9; 9-$Me_3N^+Fl^-Br^-$, 116997-73-0; $FlH_2^{\bullet+}$, 34985-70-1; 2-$MeOFlH_2^{\bullet+}$, 101631-12-3; 2,7-$(MeO)_2FlH_2^{\bullet+}$, 51548-21-1; 2-$Me_2NFlH_2^{\bullet+}$, 113533-40-7; 2,7-$(Me_2N_2)FlH_2^{\bullet+}$, 116997-74-1; 9-$Me_2NFlH^{\bullet+}$, 117065-69-7; 9-$Et_2NFlH^{\bullet+}$, 116997-75-2; 9-*i*-$Pr_2NFlH^{\bullet+}$, 116997-76-3; 9-azetidinyl-$FlH^{\bullet+}$, 116997-77-4; 2,7-$(MeO)_2$-9-pyrrolidinyl-$FlH^{\bullet+}$, 116997-78-5; 9-pyrrolidinyl-$FlH^{\bullet+}$, 116997-79-6; 9-piperidinyl-$FlH^{\bullet+}$, 116997-80-9; 9-(2,6-dimethylpiperidinyl)-$FlH^{\bullet+}$, 116997-81-0; 9-imidazolyl-$FlH^{\bullet+}$, 116997-82-1; 2,7-$(MeO)_2$-9-imidazolyl-$FlH^{\bullet+}$, 116997-83-2; 9-(2,2,6,6-tetramethyl)-FlH, 116997-84-3; 9-(2-methylpiperidinyl)FlH, 116997-85-4; 9-(3-methyl-1-pyrazolyl)FlH, 116997-86-5; 9-BrFlH, 1940-57-4; azetidine, 503-29-7.

Competing Reactions of the Acetone Cation Radical: RRKM–QET Calculations on an ab Initio Potential Energy Surface†

Nikolaus Heinrich,‡,§ Frank Louage,‖,⊥ Chava Lifshitz,*,‖ and Helmut Schwarz*,‡

Contribution from the Department of Chemistry, Technical University, D-1000 Berlin 12, F.R.G., and Department of Physical Chemistry and The Fritz Haber Research Center for Molecular Dynamics, The Hebrew University of Jerusalem, Jerusalem 91904, Israel.
Received March 21, 1988

Abstract: Two parallel unimolecular dissociations of the acetone cation radical, (1) methyl loss and (2) methane elimination, were studied by means of RRKM–QET calculations on an ab initio potential energy surface. The ab initio calculations demonstrated the existence of a hydrogen-bridged complex as an intermediate for both reaction paths. Sets of reactant and transition structure frequencies, as well as energetics based on high-level ab initio (MP3/6-31G(d,p)//6-31G(d)+ZPVE) calculations, were employed in the RRKM-QET calculations. By invoking tunneling in the CH_4 elimination channel, we were able to reproduce several experimental observations: (a) reaction channel 2 is the major channel for so-called "metastable ion" fragmentations in the microsecond lifetime range; (b) channel 1 becomes the major reaction channel at high internal energies of the reactant ion. Photoionization efficiency (PIE) curves for the two competing channels calculated on the basis of RRKM-QET microcanonical rate coefficients, $k(E)$, reproduce rather well recent experimental results by Traeger, Hudson, and McAdoo.

There have been two successful approaches in treating unimolecular fragmentations of polyatomic cations in recent years,[1] ab initio calculations of potential energy profiles and RRKM-QET calculations of microcanonical rate coefficients, $k(E)$. The latter require accurate knowledge of the energetics of the reaction in the form of the critical energy of activation, E_0, and the vibrational frequencies of the reactant and transition structures. While the vibrational frequencies of the reactant ion can be guessed, on the basis of those of the neutral molecule, and more recently there

† Dedicated to Professor F. W. McLafferty on the occasion of his 65th birthday.

‡ Technical University.
§ Permanent address: Schering AG, Section of Theoretical Chemistry, D-1000 Berlin 65, F.R.G.
‖ Hebrew University of Jerusalem.
⊥ Permanent address: Faculty of Applied Science, Vrije Universiteit Brussel, B-1050 Brussels, Belgium.

(1) Lifshitz, C. *Int. Rev. Phys. Chem.* **1987**, *6*, 35.

0002-7863/88/1510-8183$01.50/0

Scheme I

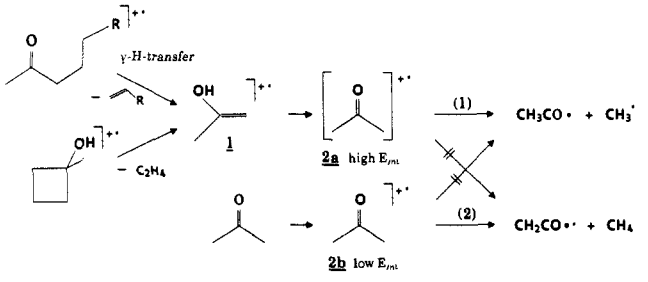

have also been some experimental measurements of vibrational frequencies of polyatomic cations,[2] those of the transition structure are unknown experimentally. The rate-energy dependence may be parametrized through the two activation parameters, the critical energy of activation, E_0, and the activation entropy, $\Delta S^{\ddagger}$.[3] On the other hand, ab initio calculations yield vibrational frequencies not only for the minima along the potential energy profile, but also for the maxima, i.e., for the transition structure configurations, which can therefore be employed for RRKM–QET calculations. We have applied this latter approach in the present study of the acetone cation radical, $C_3H_6O^{\cdot+}$.

The unimolecular chemistry of isomeric $C_3H_6O^{\cdot+}$ species in the gas phase has been the subject of continuous experimental and theoretical research over more than 15 years.[4,5] Among other isomers the tautomer pair of ionized acetone (**2**) and its enol form (**1**) has attracted particular attention for several reasons. Briefly, with respect to their relative stabilities, Holmes and Lossing[4n] were able to show that the enol form (**1**) is 14 kcal/mol more stable than ionized acetone (**2**). Based on appearance energy measurements and thermochemical data, this stability order was found for other simple ionized keto/enol pairs as well, in distinct contrast to the ordering in the respective neutral systems, where the keto forms invariably turn out to be the more stable tautomers.[6] For example, neutral acetone is by 13.9 kcal/mol more stable than 2-hydroxpropene.[7]

In 1971, McLafferty and co-workers[4d] reported the formation of **1** from higher aliphatic ketones by dissociative ionization (γ-hydrogen transfer) as well as from ionized 1-methylcyclobutanol by cycloreversion, respectively (Scheme I). They provided evidence for a rate-determining isomerization of **1** to an intermediate acetone ion **2a** prior to decomposition into $CH_3^{\cdot}$ and $C_2H_3O^+$. It is important to mention that at threshold energy there exists no evidence for a direct loss of methyl radical from **1** to generate the 1-hydroxyvinyl cation. In contrast, by means of collisional activation (CA) mass spectrometry and thermochemical data, the structure of the $C_2H_3O^+$ ion could unambiguously be determined[8,9] to uniquely correspond to the acylium ion CH_3CO^+. Based on isotopic labeling results, McLafferty and co-workers[4d] also demonstrated that the two methyl groups of intermediate **2a** were lost at unequal rates. This was later confirmed by several other groups showing that the newly formed methyl group is being lost more readily than the one originally present.[9,10] This remarkable result was suggested to be due to an incomplete energy randomization[11b] in the chemically activated acetone intermediate ion **2a** prior to decomposition. Lifshitz and co-workers[11] estimated the lifetime of the "non-ergodically" behaving ion **2a**, on the basis of the quasi-equilibrium theory (QET), to be of the order of $t \simeq 5 \times 10^{-13}$ s, hence being significantly shorter than the time normally expected for intramolecular energy redistribution (ca. 10^{-12} s).[11] In their exhaustive study, Lifshitz and Tzidony[12a] also mentioned some features of the metastable acetone radical cation **2b** directly generated by electron impact ionization of neutral acetone. Interestingly, this species gives rise predominantly to the formation of ionized ketene, $CH_2CO^{\cdot+}$, by loss of methane. This reaction, which is purely unimolecular, is connected with a narrow metastable peak of Gaussian shape. Methyl loss from the same ion was demonstrated to be due almost entirely to collision-induced dissociations,[14a] as shown by the effect of collision gas pressure. In fact, at pressure conditions of $<10^{-7}$ torr, we were unable to observe a signal corresponding to the loss of $CH_3^{\cdot}$ from ionized acetone.[12b] In summary, high-energy acetone ions **2a** (generated via isomerization of **1**) exclusively dissociate via "α-cleavage" to give $CH_3CO^+ + CH_3^{\cdot}$ (hereafter called reaction channel 1), whereas the low-energy decomposing ions **2b** only give rise to the formation of $CH_2CO^{\cdot+}$, formally via 1,2-elimination of methane (see Scheme I, reaction channel 2).

The two reaction channels 1 and 2 have been studied by photoionization mass spectrometry of acetone,[13,14a] and their appearance energies were found to be the same within experimental error, the most recent value being[14a] 10.38 eV for both processes. Nevertheless, as noted above, reaction 2 is the dominant channel for "metastable ion" fragmentations in the microsecond lifetime range, while channel 1 becomes the major reaction channel at high internal energies of photoionized acetone.[14] Competitive methyl and methane eliminations are quite general phenomena in unimolecular fragmentations of polyatomic cations and the near equality of the appearance energies for $CH_3^{\cdot}$ and CH_4 losses from the butane cation radical has been noticed by Chupka and Berkowitz as early as 1967.[15] At that time it was suggested[15] that the reactions proceed through a common intermediate. More recently,[14,16,17] McAdoo and co-workers have provided evidence that the dissociations in acetone and other ionized ketones,[14] as well as in many other systems,[16,17] are mediated by ion/neutral complexes.

In this article, we address the question related to the mechanism of $CH_3^{\cdot}$ and CH_4 losses from ionized acetone, **2b** and **2a**, respectively. Specifically, how do the two competing reaction modes

(2) Durant, J. L.; Rider, D. M.; Anderson, S. L.; Proch, F. D.; Zare, R. N. *J. Chem. Phys.* **1984**, *80*, 1817.
(3) Malinovich, Y.; Arakawa, R.; Haase, G.; Lifshitz, C. *J. Phys. Chem.* **1985**, *89*, 2253.
(4) (a) Diekman, J.; MacLeod, J. K.; Djerassi, C.; Baldeschwieler, J. D. *J. Am. Chem. Soc.* **1969**, *91*, 2069. (b) Eadon, G.; Diekman, J.; Djerassi, C. *Ibid.* **1969**, *91*, 3986. (c) Eadon, G.; Diekman, J.; Djerassi, C. *Ibid.* **1970**, *92*, 6205. (d) McLafferty, F. W.; McAdoo, D. J.; Smith, J. S.; Kornfeld, R. *Ibid.* **1971**, *93*, 3720. (e) McLafferty, F. W.; Kornfeld, R.; Haddon, W. F.; Levsen, K.; Sakai, I.; Bente, P. F.; Tsai, S.-C.; Schuddemagge, H. D. R. *Ibid.* **1973**, *95*, 3886. (f) Pritchard, J. *Org. Mass Spectrom.* **1974**, *8*, 103. (g) Beynon, J. H.; Caprioli, R. M.; Cooks, R. G. *Ibid.* **1974**, *9*, 1. (h) Conrath, K.; Van de Sande, C.; Vandewalle, M. *Ibid.* **1974**, *9*, 585. (i) Ferrer-Correia, A. J. V.; Jennings, K. R.; Sen Sharma, D. K. *J. Chem. soc., Chem. Commun.* **1975**, 973. (j) Van de Sande, C. C.; McLafferty, F. W. *J. Am. Chem. Soc.* **1975**, *97*, 4617. (k) Drewery, C. J.; Jennings, K. R. *Int. J. Mass Spectrom. Ion Phys.* **1976**, *19*, 287. (l) Ferrer-Correia, A. J. V.; Jennings, K. R.; Sen Sharma, D. K. *Org. Mass Spectrom.* **1976**, *11*, 867. (m) Luippold, D. A.; Beauchamp, J. L. *J. Phys. Chem.* **1976**, *80*, 795. (n) Holmes, J. L.; Lossing, F. P. *J. Am. Chem. Soc.* **1980**, *102*, 1591. (o) Holmes, J. L.; Lossing, F. P. *Ibid.* **1980**, *102*, 3732. (p) Terlouw, J. K.; Heerma, W.; Holmes, J. L. *Org. Mass Spectrom.* **1981**, *16*, 306. (q) Bombach, R.; Stadelmann, J. P.; Vogt, J. *Chem. Phys.* **1982**, *72*, 259. (r) Tureček, F.; McLafferty, F. W. *J. Am. Chem. Soc.* **1984**, *106*, 2528. (s) Tureček, F.; Hanus, V. *Org. Mass Spectrom.* **1984**, *19*, 631. (t) McAdoo, D. J.; Hudson, C. E. *Int. J. Mass Spectrom. Ion Processes* **1984**, *59*, 77.
(5) Bouma, W. J.; MacLeod, J. K.; Radom, L. *J. Am. Chem. Soc.* **1980**, *102*, 2246.
(6) For leading references, see: Heinrich, N.; Koch, W.; Frenking, G.; Schwarz, H. *J. Am. Chem. Soc.* **1986**, *108*, 2525.
(7) Holmes, J. L.; Lossing, F. P. *J. Am. Chem. Soc.* **1982**, *104*, 2648.
(8) Burgers, P. C.; Holmes, J. L.; Szulejko, J. E.; Mommers, A. A.; Terlouw, J. K. *Org. Mass Spectrom.* **1983**, *18*, 254.
(9) Tureček, F.; McLafferty, F. W. *J. Am. Chem. Soc.* **1984**, *106*, 2525.
(10) Depke, G.; Lifshitz, C.; Schwarz, H.; Tzidony, E. *Angew. Chem.* **1981**, *93*, 824; *Angew. Chem., Int. Ed. Engl.* **1981**, *20*, 792.
(11) (a) Oref, I.; Rabinovitch, B. S. *Acc. Chem. Res.* **1979**, *12*, 166. (b) Lifshitz, C. *J. Phys. Chem.* **1983**, *87*, 2304.
(12) (a) Lifshitz, C.; Tzidony, E. *Int. J. Mass Spectrom. Ion Phys.* **1981**, *39*, 181. (b) Schwarz, H.; Drewello, T., unpublished results.
(13) Baer, T., personal communication.
(14) (a) Traeger, J. C.; Hudson, C. E.; McAdoo, D. J. *J. Phys. Chem.* **1988**, *92*, 1519. (b) The first statement that the decompositions of ionized acetone change markedly with the internal energy was published by: McAdoo, D. J.; Witiak, D. N. *J. Chem. Soc., Perkin Trans. 2* **1981**, 770. (c) For the first suggestion that the loss of CH_4 from ionized acetone may occur through an ion/neutral complex, see: Hudson, C. E.; McAdoo, D. J. *Int. J. Mass Spectrom. Ion Processes* **1984**, *59*, 325.
(15) Chupka, W. A.; Berkowitz, J. *J. Chem. Phys.* **1967**, *47*, 2921.
(16) McAdoo, D. J.; Traeger, J. C.; Hudson, C. E.; Griffin, L. L. *J. Phys. Chem.* **1988**, *92*, 1524.
(17) McAdoo, D. J. *Mass Spectrom. Rev.* **1988**, *7*, 363.

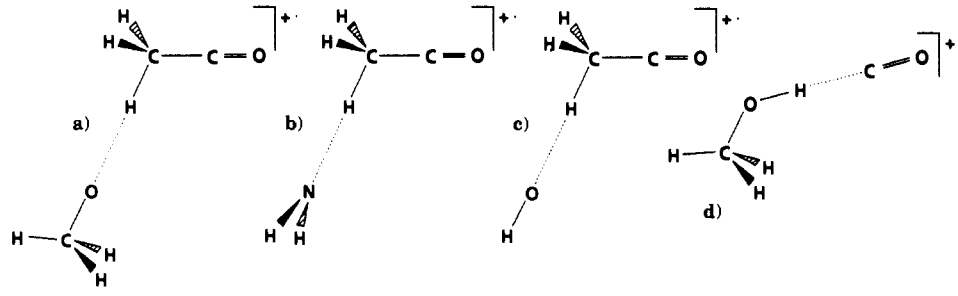

Figure 1. Selected hydrogen-bridged intermediates arising in unimolecular decompositions of methyl acetate (a), acetamide (b), acetic acid (c), and methyl formate (d). The relative stabilities toward dissociation (across the dotted line) are given in kcal/mol.

Table I. Total Energies (in Hartrees) and Zero-Points Vibrational Energies (ZPVE) (in kcal/mol) of Single Points Calculations Based on 6-31G(d) Geometries

A. 6-31G(d) Geometry

species	6-31G(d)// 6-31G(d)	6-31G(d,p)// 6-31G(d)	MP2[a]/6-31G(d,p)// 6-31G(d)	MP3[a]/6-31G(d,p)// 6-31G(d)	ZPVE (6-31G(d))[b]
1	−191.667 41	−191.683 17	−192.238 83	−192.272 08	50.0
TS **1/2**	−191.565 53	−191.580 43	−192.155 44	−192.184 17	46.2
2	−191.659 94	−191.670 66	−192.213 61	−192.252 05	49.4
TS **2/3**	−191.624 32	−191.635 43	−192.195 38	−192.220 27	45.6
3	−191.624 29	−191.635 44	−192.195 62	−192.220 49	45.7
TS **3/4**	−191.594 16	−191.606 05	−192.183 23	−192.205 65	44.3
4	−191.622 98	−191.633 60	−192.193 67	−192.219 81	45.8
CH_3CO^+	−152.059 30	−152.064 93	−152.494 88	−152.502 44	26.9
$CH_2CO^{\bullet+}$	−151.425 16	−151.429 16	−151.824 88	−151.832 96	18.6
$CH_3^\bullet$	−39.558 92	−39.564 46	−39.692 70	−39.710 17	18.7
CH_4	−40.195 17	−40.201 70	−40.364 62	−40.382 84	28.7

B. 3-21G Geometry

species	3-21G// 3-21G	6-31G(d)// 3-21G	6-31G(d,p)// 3-21G	MP2[a]/6-31G(d,p)// 3-21G	MP3[a]/6-31G(d,p)// 3-21G	ZPVE (3-21G)[b]
1	−190.595 31	−190.665 55	−191.681 19	−192.189 44	−192.219 70	51.7
TS **1/2**	−190.488 80	−191.563 06	−191.577 37	−192.105 36	−192.131 80	48.0
2	−190.588 73	−191.658 81	−191.669 49	−192.166 69	−192.156 11	52.5
TS **2/3**	−190.550 76	−191.623 42	−191.634 53	−192.152 36	−192.173 01	45.6
3	−190.551 42	−191.622 93	−191.634 16	−192.152 91	−192.173 46	47.2
TS **3/4**	−190.526 52	−191.592 71	−191.604 55	−192.137 84	−192.156 11	46.1
4	−190.548 69	−191.621 15	−191.631 77	−192.148 45	−192.170 64	45.7
CH_3CO^+	−151.201 31	−152.058 38	−152.064 01	−152.475 68	−152.480 58	26.9
$CH_2CO^{\bullet+}$	−150.569 21	−151.423 79	−151.427 76	−151.812 16	−151.818 53	18.6
$CH_3^\bullet$	−39.342 61	−39.558 99	−39.564 46	−39.668 65	−39.684 49	17.4
CH_4	−39.976 88	−40.195 17	−40.195 70	−40.332 42	−40.348 45	26.8

[a] Frozen core approximation. [b] ZPVE scaled by a factor of 0.89.

differ with respect to the intermediates involved and the respective energy requirements? In a series of recent papers we pointed to the role *hydrogen-bridged species play as intermediates* in decompositions of simple carbonyl compounds, such as methyl acetate$^{\bullet+}$,[18] acetamide$^{\bullet+}$,[19] acetic acid$^{\bullet+}$,[20] and methyl formate$^{\bullet+}$.[21] Based on ab initio molecular orbital (MO) calculations, it was demonstrated that for these systems, hydrogen-bridged ion/dipole complexes are involved in their unimolecular reactions. In fact, experimental findings like product distributions or labeling studies could only be rationalized in terms of these electrostatically bound complexes. Common to all of them, it was found that their formation can occur below their respective thresholds of decomposition. Some examples are shown in Figure 1, together with their stabilization energies toward dissociation into their components.

Among many other cases, being exhaustively reviewed by Morton in 1979[22] and, more recently, by McAdoo,[17] hydrogen-bridged intermediates have even been postulated to be involved in alkane ion decompositions[23] where the attractive forces between the ion and the polarizable component are certainly much weaker than in the examples shown in Figure 1. Do these complexes mediate the decomposition modes of ionized acetone, as well? They do, indeed, as we shall see later after briefly summarizing the computational details for a proper and economical description of the $C_3H_6O^{\bullet+}$ potential energy surface.

Ab Initio Computational Details

The ab initio MO calculations were performed using the Gaussian 82[24] and GAMESS[25] programs running on CRAY-XMP and Cyber CDC 175 computers, respectively. All open-shell species were treated within the unrestricted Hartree–Fock (UHF) formalism.[26] The expectation values

(18) Heinrich, N.; Schmidt, J.; Schwarz, H.; Apeloig, Y. *J. Am. Chem. Soc.* **1987**, *109*, 1317.
(19) Drewello, T.; Heinrich, N.; Maas, W. P. M.; Nibbering, N. M. M.; Weiske, T.; Schwarz, H. *J. Am. Chem. Soc.* **1987**, *109*, 4810.
(20) Heinrich, N.; Schwarz, H. *Int. J. Mass Spectrom. Ion Processes* **1987**, *79*, 295.
(21) Drewello, T.; Heinrich, N.; Morrow, J. C.; Schmidt, J.; Schwarz, H., manuscript in preparation.
(22) Morton, T. H. *Tetrahedron* **1982**, *38*, 3195.
(23) Wendelboe, J. F.; Bowen, R. D.; Williams, D. H. *J. Am. Chem. Soc.* **1981**, *103*, 2333 and references cited therein.
(24) Binkley, J. S.; Frisch, M. J.; DeFrees, D. J.; Raghavachari, K.; Whiteside, R. A.; Schlegel, H. B.; Fluder, E. M.; Pople, J. A. *Carnegie*-Mellon University, Pittsburgh, PA, 1984, Rev. H.

Table II. Relative Energies (kcal/mol) on Selected Levels of Theory

species	3-21G// 3-21G	6-31G(d)// 3-21G	6-31G(d)// 6-31G(d)	6-31G(d,p)// 6-31G(d)	MP3/6-31G(d,p)// 3-21G + ZPVE	MP3/6-31G(d,p)// 6-31G(d) + ZPVE	exptl
1	−4.1	−7.4	−4.7	−7.9	−14.5	−12.0	−14
TS **1/2**	62.9	57.9	59.3	56.7	37.7	39.4	32, 41
2	0.0	0.0	0.0	0.0	0.0	0.0	0
TS **2/3**	23.9	21.9	22.4	22.1	11.4	16.1	
3	23.5	22.2	22.4	22.1	12.7	16.1	
TS **3/4**	39.1	30.8	41.3	30.6	22.1	24.0	
4	25.2	23.7	33.2	23.2	13.3	16.8	
$CH_2CO^{\bullet+} + CH_4$	26.5	28.9	24.9	25.0	19.1	20.6	19
$CH_3CO^+ + CH_3^\bullet$	28.2	25.7	26.2	25.9	18.4	21.0	19

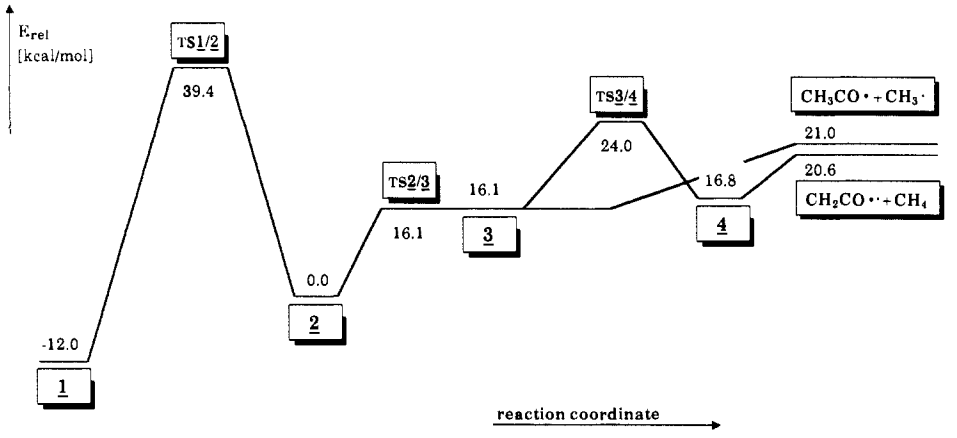

Figure 2. Schematic potential energy diagram (MP3/6-31G(d,p)//6-31G (d) + ZPVE).

for the S^2 operator were always very close to the value of 0.75 for the pure spin state, i.e., in a range of 0.75 to 0.78. Thus, the UHF wave function serves as a good approximative function for the pure doublet state. All structures have been optimized using a polarized 6-31G(d) basis set.[27] The stationary points were characterized by calculating the analytical harmonic force constant matrix at the same level of theory; local minima have no negative eigenvalues while transition structures correspond to one and only one negative eigenvalue. For the calculation of zero-point vibrational energies (ZPVE), the vibrational frequencies have been scaled by a factor of 0.89 to account for their systematic overestimation at the Hartree–Fock level.[28] For stationary points, single point calculations have been performed with a 6-31G(d,p) basis set;[27] this basis set was also used for calculations aimed at accounting for the effects of valence electron correlation by means of Møller–Plesset perturbation theory[29] terminated at third order (MP3). Thus, the highest level of theory discussed within the text refers to MP3/6-31G(p,d)//6-31G(d) + ZPVE, if not stated otherwise. From preliminary computations[30] we also include for comparison some results which are based on 3-21G[31] geometries. Single point calculations with extended basis sets including electron correlation effects have also been performed. The MP3/6-31G(d,p)//3-21G energies were obtained using the additivity scheme[32] for the polarization functions on hydrogen, using the following approximation:

$$E(\text{MP3/6-31G(d,p)}) = E(\text{MP3/6-31G(d)}) + E(\text{HF/6-31G(d,p)}) - E(\text{HF/6-31G(d)})$$

Total energies are given in Table I; relative energies are collected in Table II, together with experimental data derived from known heats of formation or appearance energy measurements. The optimized geometries are given in Chart I (bond lengths in Å, bond angles in degrees); Figure 2 provides a schematic of the potential energy diagram.

Results and Discussion of the ab Initio Calculations

At the 6-31G(d) level of theory, the acetone ion **2** has been found to have C_2 symmetry with the two methyl groups being about 10° rotated out of the C–O plane. The C_{2v} structure was found to be less than 0.1 kcal/mol higher in energy, and the normal mode corresponding to methyl rotation has a small imaginary frequency of 49 cm^{-1}. However, if zero-point vibrational energies are taken into account, the two species become isoenergetic since the differences in total energies are counterbalanced by the differences in ZPVE.

We elongated one C–C bond systematically in steps of 0.1 Å by optimizing all other geometry parameters imposing C_s symmetry to simulate the minimal energy reaction path (MERP) for α-cleavage. After a steep increase in the potential energy, reflecting the loss of covalent interaction, the methyl moiety was found to migrate along the positively charged rod of the acylium ion attracted by purely electrostatic interactions, about 5 kcal/mol below the combined energies of the separated products, CH_3CO^+ and $CH_3^\bullet$. The surface in that region turns out to be extremely flat, and significant geometrical changes exert practically negligible effects on the total energies. Note that even at a mean distance of 3–3.5 Å from the acylium ion the migrating methyl radical is slightly pyramidalized (C_{3v} symmetry), about 7° distorted from planarity, reflecting the induced dipolar interaction. Isolated CH_3 radicals are known to have D_{3h} symmetry.[33] The transition structure for the methyl migration, TS **2/3** was found to have an extremely low imaginary frequency of 25 cm^{-1} in the normal modes. Whether or not this structure corresponds to a distinguished point on the surface is certainly of minor interest in the present context.[60] It is much more important to realize that about 16 kcal/mol above the covalently bound acetone ion **2**, and still 5 kcal/mol below the dissociation limit, various conformations of the ion/neutral complex $[CH_3CO^+/CH_3^\bullet]$ may freely interconvert within a few tenths of a kilocalorie.

With regard to the formation of ionized ketene and CH_4, hydrogen transfer must eventually occur, and, therefore, structure **3** can be viewed as a reasonable conformation within the set of

(25) Dupuis, M.; Spangler, D.; Wenddoski, J. J. NRCC Program QG 01, 1980; modifications by J. van Lenthe, Utrecht (NL), 1985.
(26) Pople, J. A.; Nesbet, R. K. *J. Chem. Phys.* **1954**, *22*, 57.
(27) Hariharan, P. C.; Pople, J. A. *Theor. Chim. Acta* **1972**, *28*, 213.
(28) Pople, J. A.; Schlegel, H. B.; Krishnan, R.; DeFrees, D. J.; Binkley, J. S.; Frisch, M. J.; Whiteside, R. A.; Hout, R. F.; Hehre, W. J. *Int. J. Quantum Chem. Symp.* **1981**, *15*, 269.
(29) Møller, C.; Plesset, M. S. *Phys. Rev.* **1934**, *46*, 618.
(30) Heinrich, N. Ph.D. Thesis D83, Technical University Berlin, 1987.
(31) Binkley, J. S.; Pople, J. A.; Hehre, W. J. *J. Am. Chem. Soc.* **1980**, *102*, 939.
(32) Nobes, R. H.; Bouma, W. J.; Radom, L. *Chem. Phys. Lett.* **1982**, *89*, 497.

(33) See: Chau, F. T. *J. Mol. Struct. (THEOCHEM)* **1985**, *119*, 281 and references therein.

Chart I. 6-31G(d) Optimized Geometries[a]

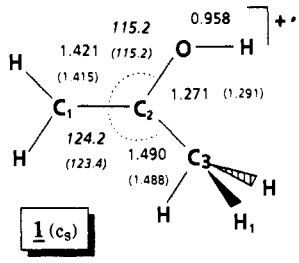

1 (C_s)

Atom charges		Spin density	
C_1	-0.20	C_1	0.91
C_2	+0.51	C_2	0.09
C_3	-0.45	O	0.21
O	-0.46		

$\measuredangle H_1C_3C_2O$ 59.2° (59.8°)

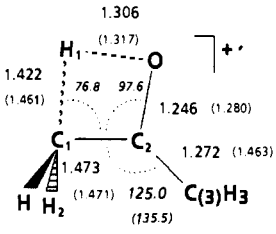

TS1/2 (C_s)

Atom charges		Spin density	
C_1	-0.43	C_1	0.90
C_2	+0.62	C_2	-0.10
C_3	-0.45	O	0.79
O	-0.36	H_1	-0.14
H_1	+0.35		

$\measuredangle H_2C_1C_2O$ 103.7° (102.4°)

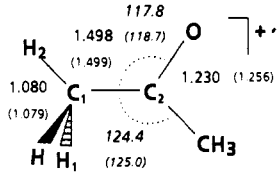

2 (C_2)

Atom charges		Spin density	
C_1	-0.43	C_2	-0.20
C_2	+0.50	O	1.18
O	-0.07		
H_1	+0.24		

$\measuredangle H_1C_1C_2O$ 110.5° (121.6°)
$\measuredangle H_2C_1C_2O$ -10.1° (0.0°)

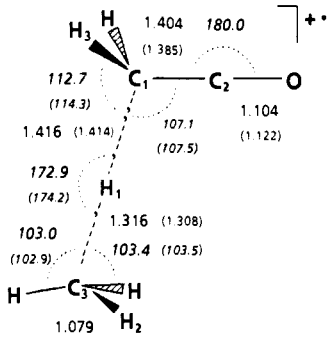

TS3/4 (C_s)

Atom charges		Spin density	
C_1	-0.42	C_1	0.81
C_2	+0.72	C_2	-0.02
C_3	-0.39	C_3	0.60
O	-0.20	O	0.20
H_1	+0.08	H_1	-0.19

$\measuredangle H_2C_3C_1C_2$ 67.1° (60.1°)
$\measuredangle H_3C_1C_2C_3$ 119.8° (111.4°)

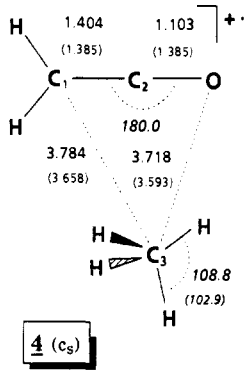

4 (C_s)

Atom charges		Spin density	
C_1	-0.19	C_1	1.03
C_2	+0.70	C_2	-0.18
C_3	-0.51	O	0.39
O	-0.15		

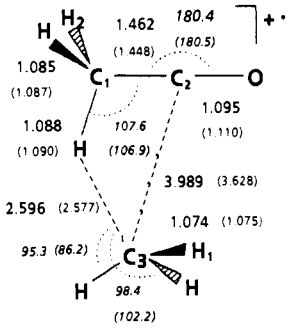

TS2/3 (C_s)

Atom charges		Spin density	
C_1	-0.45	C_3	1.24
C_2	+0.72		
C_3	-0.44		
O	-0.16		

$\measuredangle H_1C_3C_2C_1$ 119.7° (94.3°)
$\measuredangle H_2C_1C_2C_3$ 120.0° (118.6°)

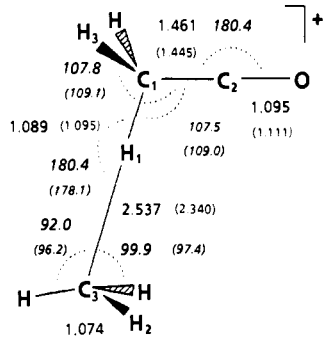

3 (C_s)

Atom charges		Spin density	
C_1	-0.45	C_3	1.22
C_2	+0.72		
C_3	-0.44		
O	-0.16		
H_1	+0.28		
H_2	+0.29		
H_3	+0.28		

$\measuredangle H_2C_3C_1C_2$ -60.2° (-60.7°)
$\measuredangle H_2C_1C_2C_3$ 120.0° (119.1°)

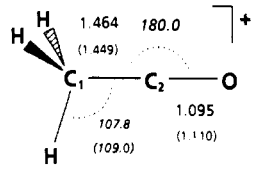

(C_{3v})

Atom charges
C_1 -0.44
C_2 +0.72
O -0.16
H +0.29

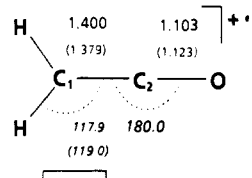

(C_{2v})

Atom charges		Spin density	
C_1	-0.44	C_1	1.02
C_2	+0.72	C_2	-0.18
O	-0.16	O	0.39
H	+0.32		

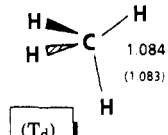

(T_d)

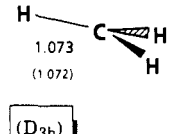

(D_{3h})

[a] Bond lengths are given in Å and bond angles in degrees. 3-21G data are given in parentheses.

ion/neutral species; moreover, **3** may provide a maximum orbital overlap for subsequent C–H bond formation. The force constant matrix of **3** turns out to have only positive eigenvalues and the lowest frequency of the normal modes (8 cm^{-1}, a'') corresponds to methyl rotation around the C–H–C bridge rather than to a CH_3 shift. Note, that the hydrogen bridge has an almost linear ge-

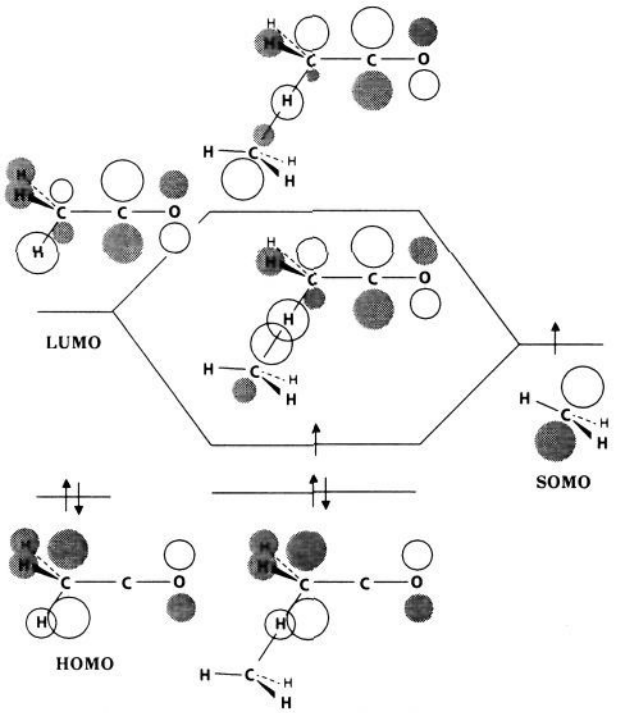

Figure 3. Schematic orbital interaction for TS **3/4**.

ometry. For hydrogen transfer, i.e., covalent bond formation, the two components come much closer together; the C–C distance in the hydrogen bridge of structure **3**, 3.626 Å, is dramatically shortened to 2.732 Å in the transition structure TS **3/4**. The two critical C–H distances (see Chart I) indicate a covalent binding of the transition structure and are very similar to those known for "conventional" [1.2] or [1.3] hydrogen shifts.[30]

In terms of a simple perturbational group orbital approach, the H-transfer is governed by a one-electron/two-orbital interaction between the singly occupied hybride orbital of $CH_3^\bullet$ (SOMO) and the doubly occupied, C–H antibonding orbital of the acylium ion (LUMO) as shown in Figure 3. Hydrogen transfer leads to a weakly bound complex between ionized ketene and neutral methane, e.g., **4**, which is stabilized by 3.8 kcal/mol toward decomposition into its components.

Alternatively, the hydrogen-bridged intermediate **3** may decompose into its components, CH_3CO^+ and $CH_3^\bullet$, in a continuously endothermic process.

Before we turn to a discussion of the theoretical results in light of the experimental findings, a comment has to be made on the theoretical models used in this study. It is well known that much theoretical effort has to be spent for a proper description of hydrogen-bridged or, more generally speaking, electrostatically bound species. Comparative studies on cationic hydrogen-bridged dimers of the type $(AH_n)_2H^+$ by Del Bene and co-workers,[34] as well as the growing number of papers dealing with van der Waals type complexes,[35] convincingly demonstrate the importance of flexible basis sets for a proper geometry optimization. Here, the inclusion of polarization functions turns out to be of crucial importance. Basis sets of valence double-ζ quality augmented by two sets of polarization functions, as the 6-31G(1p,2d) and 6-31G(2p,2d) basis sets,[36] have been shown to describe electric properties such as dipole and quadrupole moments quite well.[37] It was also shown that the inclusion of electron correlation is necessary for getting reasonable interaction energies.[34,37] Minimal split valence basis sets,

Scheme II

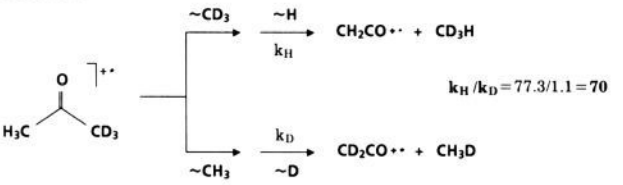

such as 3-21G, tend to overestimate electrostatic attractions.[38] This has consequences for the interaction energy itself as well as for the respective geometries, which come out too tightly bound. The polarized 6-31G(d) basis can be viewed as a good compromise between offering optimal flexibility of the basis set used and computer time. The 6-31G(d) basis set is superior to the 3-21G basis set, but the latter is well suited at least for a qualitative insight, and, of course, it serves well as a reasonable starting point for higher level calculations. The comparison of the structures TS **2/3**, **3**, TS **3/4**, and **4**, optimized with the two basis sets, might give an impression about the range of geometry changes obtained upon basis set extension. A comparison of the relative energies obtained at MP3/6-31G(d,p)//6-31G(d) + ZPVE and MP3/6-31G(d,p)//3-21G + ZPVE (using the additivity scheme defined above) indicates that at both levels of theory the qualitative picture is almost identical. The thermochemistry for both reaction modes is in good agreement with the experimental values (see Table II) derived from the respective heats of formation. Note, however, that the ordering of the two decomposition product pairs is reversed if the energies, based on 3-21G geometry, are considered. The effect of electron correlation is most pronounced for the transition structure TS **3/4**. At the Hartree–Fock/6-31G(d,p)//6-31G(d) level, an activation energy of about 40 kcal/mol relative to the acetone ion has been obtained. This barrier is decreased by more than 20 kcal/mol at the highest level of theory; this range is typical for correlation effects in transition structures involving hydrogen migrations.[30]

It should be mentioned that we did not correct our results for basis set superposition errors (BSSE),[39] which are expected to affect the interaction in electrostatically bound species. However, it has been shown[37,40] that these effects, though they tend to overestimate the complex stability, are not very pronounced and do not exceed 1–2 kcal/mol.

Does the theoretical picture match the experimental findings? For the CH_4 loss, the calculations at each level of theory predict the hydrogen transfer via TS **3/4** to be rate determining. At the highest level of theory, TS **3/4** is 3.4 kcal/mol above the dissociation products $CH_2CO^{\bullet+}$ and CH_4. $CH_3^\bullet$ loss occurs continuously endothermic from species **3**. The dissociation products are 3.0 kcal/mol *below* TS **3/4**. However, according to the experimental findings, only CH_4 loss has been observed for metastable ions. While this reaction is slightly less endothermic than the elimination of $CH_3^\bullet$, it is kinetically disfavored due to the barrier associated with the former process.

In order to solve this problem, we have performed calculations on the unimolecular rate constant, $k(E)$, by using RRKM theory.[1,2] In addition, the possibility of a hydrogen transfer via quantum-mechanical tunneling has been considered. This possibility, aimed at resolving the discrepancies between experiment and theory, was based on the observation of an unusually large isotope effect associated with methane loss from D_3-labeled acetone, as reported earlier by Lifshitz and Tzidony.[12] Their experimental findings are summarized in Scheme II.

(34) Del Bene, J. E.; Frisch, M. J.; Pople, J. A. *J. Phys. Chem.* **1985**, *89*, 3664, 3669 and literature therein.
(35) For a review, see: Beyer, A.; Karpfen, A.; Schuster, P. *Top. Curr. Chem.* **1984**, *120*. 1.
(36) van Duijneveldt-van de Rijdt, J. G. C. M.; van Duijneveldt, F. B. *J. Mol. Struct.* **1982**, *89*, 185.
(37) Latajka, Z.; Scheiner, S. *Chem. Phys.* **1985**, *98*, 59.
(38) Hozba, P.; Schneider, B.; Carsky, P.; Zahradnik, R. *J. Mol. Struct. (THEOCHEM)* **1986**, *138*, 377.
(39) For a selected list of examples, see: (a) Urban, M.; Hobza, P. *Theor. Chim. Acta* **1975**, *207*, 215. (b) Ostlund, N. S.; Merrifield, D. L. *Chem. Phys. Lett.* **1976**, *39*, 612. (c) Bulski, H.; Chalasinski, G. *Theor. Chim. Acta* **1977**, *44*, 399. (d) Kolos, W. *Ibid.* **1979**, *51*, 219. (e) Leclercq, J. M.; Allavena, M.; Bouteiller, Y. *J. Chem. Phys.* **1983**, *78*, 4606. (f) Hobza, P.; Zahradnik, R. *Int. J. Quantum Chem.* **1983**, *23*, 325. (g) Wells, B. H.; Wilson, S. *Chem. Phys. Lett.* **1983**, *101*, 429.
(40) Postma, R.; Ruttink, P.J.A.; van Baar, B.; Terlouw, J. K.; Holmes, J. L.; Burgers, P. C. *Chem. Phys. Lett.* **1986**, *123*, 409.

Table III. Parameters Employed in RRKM-QET Calculations

	vib freq (cm^{-1})	endothermicities (kcal/mol)	critical energies of activation (kcal/mol)	activation entropies (1000 K) (eu)
reactant ion	3354, 3354, 3302, 3296, 3218, 3212, 1699, 1603, 1594, 1577, 1565, 1515, 1490, 1310, 1210, 1175, 1021, 977, 804, 502, 463, 368, 113, 77			
reaction 1 TS, calcd (a)	3439, 3439, 3314, 3278, 3270, 3168, 2626, 1552, 1551, 1544, 1544, 1526, 1168, 1166, 854, 809, 456, 448, 233, 216, 135, 57, 20	21	21	11.5
reaction 1 TS, calcd (b)	3439, 3439, 3314, 3278, 3270, 3168, 2626, 1552, 1551, 1544, 1544, 1526, 1168, 1166, 854, 809, 456, 448, 233, 216, 135, 30, 8			14.6
reaction 2 TS **3/4**	3404, 3404, 3390, 3287, 3253, 2517, 1560, 1558, 1532, 1434, 1406, 1381, 1191, 1120, 1023, 781, 689, 496, 463, 436, 368, 119, 38 imaginary frequency: 1634	20.6	24 (relative to acetone well) $V_1 = 7.3$, $V_2 = 7.2$ } Eckart potential barrier	3.94

Possible contributions of secondary isotope effects on the product distributions should be very small because hybridization of the methyl carbon is not changed during migration and subsequent hydrogen transfer; i.e., local C_{3v} symmetry in the methyl group is retained in the whole reaction sequence. The measured value of $k_H/k_D = 70$, therefore, reflects largely the primary isotope effect associated in the hydrogen-transfer step. Primary isotope effects, however, only occasionally exceed values of 3–5 in "conventional", i.e., classical hydrogen-transfer reactions.[41] Two chemically feasible effects may account for the unusual observation in the case of D_3 labeled acetone: Firstly, isotope effects may increase exponentially if the excess energy range ($E - E_0$) of the process becomes very narrow.[42] Secondly, quantum-mechanical tunneling through a potential energy barrier is accompanied by large primary isotope effects.[43] We have calculated the rate constants for both loss of $CH_3^\bullet$ and CH_4 by taking into account the tunneling probability. The results will be described in the next section.

RRKM-QET Computational Details

Assumptions made and data used in the calculations are as follows. (1) Dissociation takes place from the acetone cation radical potential well; i.e., the reactant, even if going through the H-bridged complex, has available to it the high density of states of the acetone well (Figure 2). (2) The energetics of the dissociations conform to those of the highest level ab initio calculations (Figure 2), MP3/6-31G(d,p)//6-31G(d) + ZPVE. This leads to the endothermicities, ΔH, and critical activation energies (at 0 K), E_0, as summarized in Table III. (3) Reaction 2 can take place at its endothermic threshold by quantum-mechanical tunneling through the barrier. An unsymmetrical Eckart barrier has been assumed[44,45] with tunneling taking place between the H-bridged complex **3** and the ketene ion/methane complex **4**, and thus the heights adopted for the Eckart barrier are $V_1 = 7.9$ kcal/mol and $V_2 = 7.2$ kcal/mol, respectively. The imaginary frequency necessary for the calculation was taken from the ab initio calculations to be 1634 cm^{-1}. (4) Reactant frequencies were taken equal to the ones calculated ab initio for the acetone cation radical (Table III). Transition-state frequencies for reaction 2 were taken from the ab initio calculations for the H-transfer transition structure (Table III) since TS **3/4** is rate determining. These frequencies lead to an equivalent 1000 K activation entropy for reation 2, $\Delta S^\ddagger$ (1000 K) = 3.94 eu. Transition structure frequencies for reaction 1 were chosen in two alternative ways. (a) The vibrational frequencies calculated ab initio for the H-bridged complex were adopted. One of these, 115 cm^{-1}, the C–H–C stretching mode, was chosen as the reaction coordinate. Two others, the CH_3 rotation around the C–H–C bridge and the CH_3 shift to get acetone, which are 30 and 8 cm^{-1} in the hydrogen-bridged complex, were slightly varied to reach an activation

Table IV. Tunneling Probabilities for Reaction 2

E (kcal/mol)	$\mathcal{H}(E)$ tunneling probability	E (kcal/mol)	$\mathcal{H}(E)$ tunneling probability
20.6	6.61×10^{-3}	22.5	1.32×10^{-1}
20.7	7.91×10^{-3}	23.0	2.41×10^{-1}
20.8	9.44×10^{-3}	23.5	3.92×10^{-1}
20.9	1.12×10^{-2}	24.0	5.61×10^{-1}
21.0	1.34×10^{-2}	24.5	7.12×10^{-1}
21.5	3.06×10^{-2}	25.0	8.15×10^{-1}
22.0	6.58×10^{-2}	25.5	8.98×10^{-1}

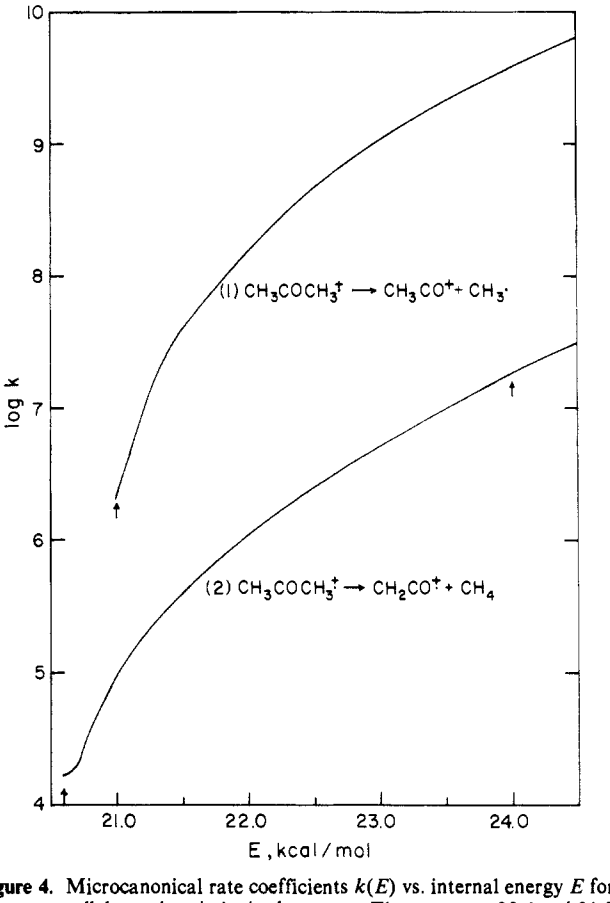

Figure 4. Microcanonical rate coefficients $k(E)$ vs. internal energy E for the two parallel reactions in ionized acetone. The arrows at 20.6 and 21.0 kcal/mol are the endothermicity thresholds for reactions 2 and 1, respectively; the arrow at 24.0 kcal/mol is the height of barrier for reaction 2 (TS **3/4**).

(41) Weiske, T.; Halim, H.; Schwarz, H. *Chem. Ber.* **1985**, *118*, 495 and references cited therein.
(42) Robinson, P. J.; Holbrook, K. A. *Unimolecular Reactions*; Wiley: London, 1972.
(43) (a) Cooks, R. G.; Beynon, J. H.; Caprioli, R. M.; Lester, G. R. *Metastable Ions*; Elsevier: Amsterdam, 1973. (b) Levsen, K. *Fundamental Aspects of Organic Mass Spectrometry*; Verlag Chemie: Weinheim, 1978.
(44) Johnston, H. S. *Gas Phase Reaction Rate Theory*; Ronald Press: New York, 1966.
(45) Eyring, H.; Walter, J.; Kimball, G. E. *Quantum Chemistry*; Wiley: New York, 1944.

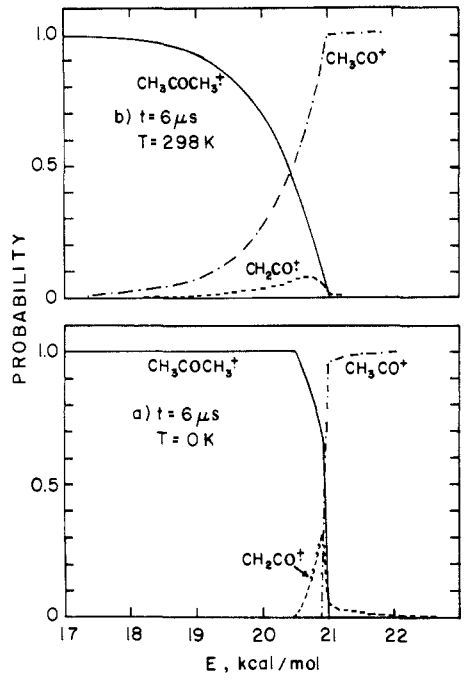

Figure 5. Calculated breakdown curves for t = 6 μs: (a) 0 K, (b) 298 K. The fractional abundances (probabilities) of the parent ion $CH_3COCH_3^{\cdot+}$, acetyl, CH_3CO^+, and ionized ketene, $CH_2CO^{\cdot+}$, are plotted as a function of the energy transferred upon ionization.

entropy, $\Delta S^{\ddagger}$ (1000 K) = 11.5 eu, equal to the one for the analogous reaction in neutral acetone.[46] The resultant frequencies are summarized in Table III. (b) One frequency (115 cm^{-1}) was removed from the frequencies of the H-bridged complex with no further changes. These frequencies (Table III) correspond to $\Delta S^{\ddagger}$ (1000 K) = 14.6 eu.

The microcanonical rate coefficient $k(E)$ for reaction 2 was calculated for energies $E' \geq 4.5$ kcal/mol above the hydrogen-bridged complex, using expression I[47] ($E = E' + 16.1$ kcal/mol, see Figure 2)

$$k(E) = 2 \frac{\sum_{e=20.6}^{E} \kappa(e) P^{\ddagger}(E - e)}{h\rho(E)} \qquad (I)$$

where $\kappa(e)$ is the tunneling probability for a one-dimensional motion with energy e along the reaction coordinate, $P^{\ddagger}(E - e)$ is the number of vibrational states for the transition structure at energy $E - e$, h is Planck's constant, $\rho(E)$ is the density of states of acetone cation radical, and the factor 2 is the reaction path degeneracy.

Results and Discussion of the RRKM–QET Calculations

(1) $k(E)$ Calculations. The tunneling probabilities calculated for reaction 2 are summarized in Table IV, as a function of the internal energy, E, in the acetone radical cation. These tunneling probabilities allow reaction channel 2 (the methane elimination) to take place via the H-bridged complex, below the energy barrier for the TS 3/4. The resultant microcanonical rate coefficients for the two parallel reaction channels (1 and 2) of the acetone radical cation are reproduced in Figure 4.

Between the two endothermicity limits 20.6 and 21.0 kcal/mol for reactions 2 and 1, respectively, reaction 2, the methane elimination, is the only reaction taking place. Furthermore, its calculated microcanonical rate coefficients are in the range $1.7 \times 10^4 - 9.5 \times 10^4$ for the energy range 20.6–21.0 kcal/mol. It is thus not surprising that a metastable ion is observed for it. This metastable dissociation can take place only over a very limited energy range (0.4 kcal/mol), since at the threshold for channel 1, the methyl loss channel is 23 times faster than the methane elimination, which from that point onward, with increasing energies, is completely suppressed. The $k(E)$ curve for reaction 2, at E = 24.0 kcal/mol (the TS 3/4 barrier height), is already at

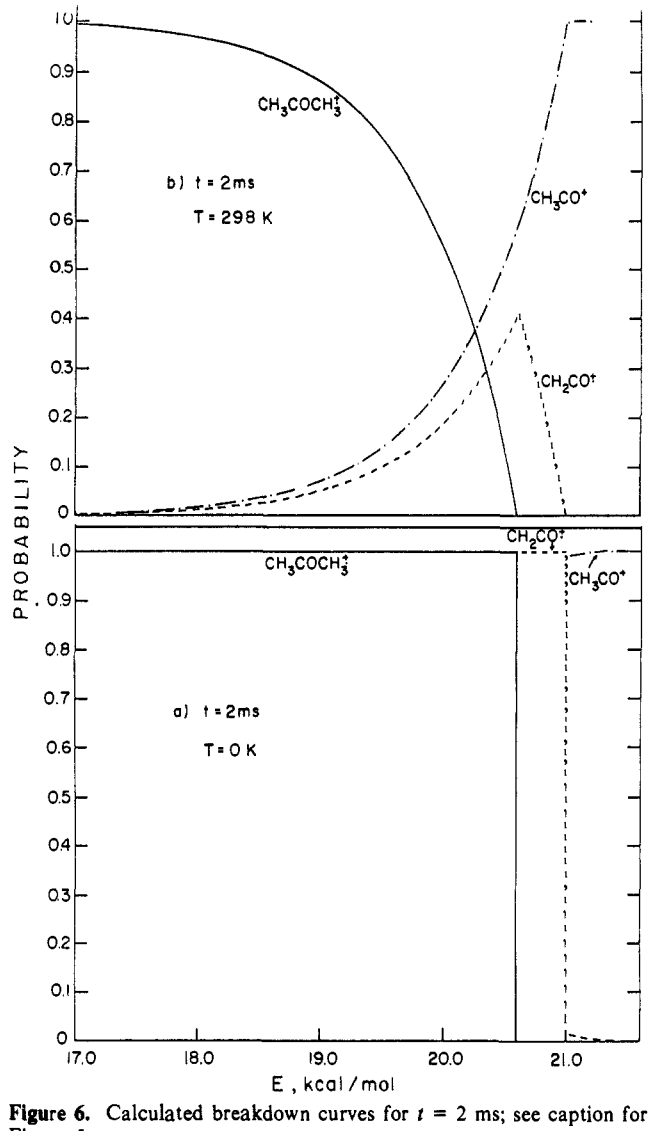

Figure 6. Calculated breakdown curves for t = 2 ms; see caption for Figure 5.

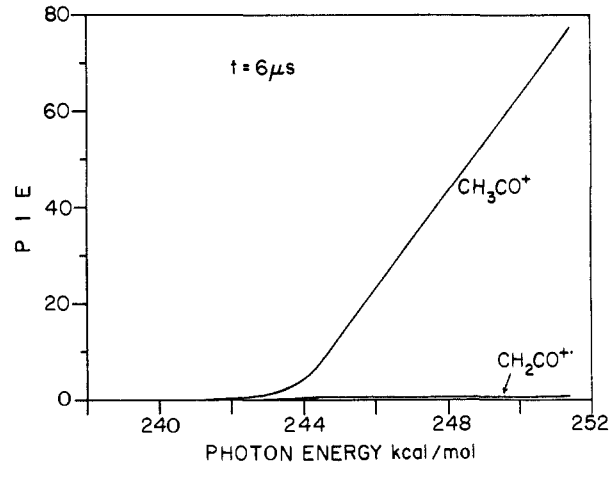

Figure 7. Calculated PIE (photoionization efficiency) curves (PIE vs. photon energy in kcal/mol) for CH_3CO^+ and $CH_2CO^{\cdot+}$ at t = 6 μs.

(46) Benson, S. W.; O'Neal, H. E. *Kinetic Data on Gas Phase Unimolecular Reactions*, NSRDS-NBS 21; National Bureau of Standards: Washington, D.C., 1970; p 416.

(47) (a) Miller, W. H. *J. Am. Chem. Soc.* **1979**, *101*, 6810. (b) Osamura, Y.; Schaefer, H. F., III; Gray, S. K.; Miller, W. H. *Ibid.* **1981**, *103*, 1904.

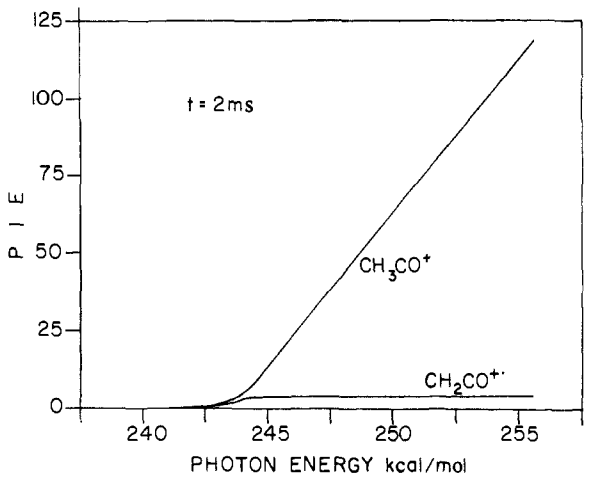

Figure 8. Calculated PIE curves for CH_3CO^+ and $CH_2CO^{+\cdot}$ at t = 2 ms.

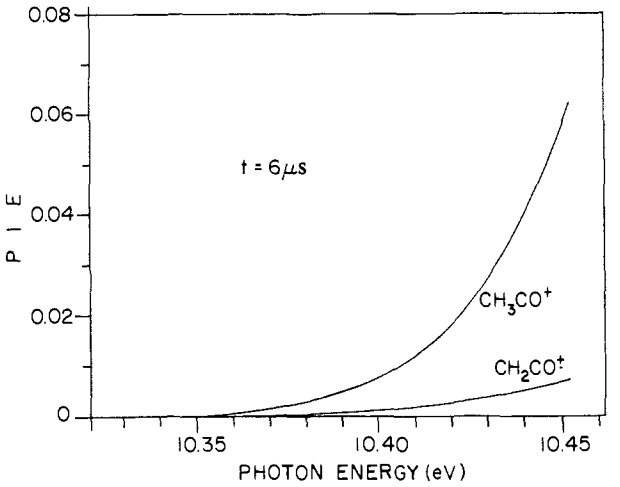

Figure 9. Threshold region of Figure 7 on an expanded PIE scale; the photon energy scale is in eV.

a point where the two reaction rates differ by more than two orders of magnitude. It is clear that very little dissociation in the metastable range is to be expected for reaction 1, since even for the model a calculation $k(E)$ rises from 2.2×10^6 at threshold to 1.7×10^7 s^{-1} within 0.3 kcal/mol. For higher activation entropies, e.g., model b (Table III), $k(E)$ rises to 1.2×10^7 s^{-1} within 0.1 kcal/mol above threshold. Model a corresponds to a preexponential A factor, for the thermal Arrhenius-type expression of the rate constant, for reaction 1, $A = (k_B T/\hbar)e^{\Delta S^{\ddagger}/R}$, ($k_B$ = Boltzmann constant, $\hbar$ = Planck's constant, R = gas constant) such that log A (1000 K) = 16.26. This corresponds to a totally loose transition structure for reaction 1 ("orbiting" transition structure), since (1) is continuously endothermic and its reverse reaction possesses no activation barrier.

(2) Breakdown Curve Calculations. The breakdown curve of an ion gives its fractional abundance as a function of the internal energy in the parent molecular ion or as a function of the energy transferred in the ionization process. At 0 K the transferred energy is equal to the internal energy (plus the adiabatic ionization energy). At 298 K, the internal energy consists of the thermal energy of the neutral molecule plus the transferred energy. Breakdown curves were calculated on the basis of first-order kinetics, at 0 K from the microcanonical rate coefficients, according to the expressions

$$\mathrm{FA}(CH_3CO^+) = \frac{k_1(E)}{k_1(E) + k_2(E)}\left[1 - e^{-[k_1(E)+k_2(E)]t}\right] \quad \text{(II)}$$

$$\mathrm{FA}(CH_2CO^{+\cdot}) = \frac{k_2(E)}{k_1(E) + k_2(E)}\left[1 - e^{-[k_1(E)+k_2(E)]t}\right] \quad \text{(III)}$$

$$\mathrm{FA}(CH_2CO^{+\cdot}) = \frac{k_2(E)}{k_1(E) + k_2(E)}\left[1 - e^{-[k_1(E)+k_2(E)]t}\right] \quad \text{(IV)}$$

where FA stands for fractional abundance and t is the reaction time. Breakdown curves were calculated at 298 K by convolution of the 0 K curves with the thermal energy distribution calculated from the vibrational frequencies of neutral acetone. The resultant breakdown curves at two reaction times, t = 6 μs and t = 2 ms, are represented in Figures 5 and 6, respectively.

There are several significant results. (i) At 0 K, as expected, there are finite values for the breakdown curve of $CH_2CO^{+\cdot}$ for E = 20.6 - 20.9 kcal/mol, but those for CH_3CO^+ are 0. (ii) Once E = 21.0 kcal/mol there is an almost immediate jump in the breakdown curve of CH_3CO^+ to 1 and that for $CH_2CO^{+\cdot}$ drops to nearly 0. (iii) A strong reaction-time effect is predicted which still needs to be corroborated by an independent experiment.[48] At 6 μs, the $CH_2CO^{+\cdot}$ fractional abundance reaches a maximum of 0.3 at 20.9 kcal/mol; at 2 ms it has a value of 1.0 for 20.6–20.9 kcal/mol. (iv) Perhaps most significant is the temperature effect; it completely washes out the slightly lower energy onset of $CH_2CO^{+\cdot}$ at 0 K. At 2 ms and 298 K the thresholds for reactions 1 and 2 are about the same while at 6 μs and 298 K the threshold is, in fact, lower for CH_3CO^+ than for $CH_2CO^{+\cdot}$. (v) Finally, CH_3CO^+ is the dominant ion at high energies.

(3) Calculation of Photoionization Efficiency Curves. Photoionization efficiency (PIE) curves were calculated for comparison with experimental ones by Traeger et al.[14] The PIE curves were calculated from the daughter breakdown curves by integration following convolution with the threshold photoelectron spectrum (TPES). The TPES is almost flat in the energy range of interest,[49] near the onsets of dissociation via reactions 1 and 2, and convolution was carried out with a flat TPES.

PIE curves were calculated for 6 μs and 2 ms, respectively. Results are shown in Figures 7–9. The following are some conclusions.

(i) The overall experimental data of Figure 1 in ref 14a are reproduced rather well by Figures 7 and 8. (ii) A strong time effect favoring CH_4 formation at long reaction times is predicted, which needs to be pursued experimentally.[48] (iii) The expanded intensity range near threshold (Figure 9) demonstrates an appearance energy (AE) in rather good agreement with experiment (calculated AE for CH_3CO^+ = 10.36 eV; lit. values: 10.33,[50] 10.37,[51] 10.38,[14,52] and 10.42 eV[53]). It is clear that this low value is due to the effect of thermal energy, and indeed molecular beam photoionization of cooled acetone gave a considerably higher value: AE = 10.52 ± 0.02 eV[54] in fair agreement with the ab initio calculation (Figure 2) which predicts a 0 K appearance energy for CH_3CO^+ of 10.6 eV (based on the ionization energy of acetone, $IE(CH_3COCH_3)$ = 9.694 ± 0.006 eV[54] and on the critical energy for reaction 1, 21.0 kcal/mol). No experimental value is available, to the best of our knowledge, for $AE(CH_2CO^{+\cdot})$ from molecular beam photoionization of cooled acetone. At 298 K the two AE's for CH_3CO^+ and $CH_2CO^{+\cdot}$ are equal (Figure 9) to within the experimentally observed accuracy.[14]

Conclusions

Statistical theory calculations such as RRKM–QET can be performed on an ab initio surface, yielding agreement with experimental observations for competitive reactions of polyatomic cations. The formation of intermediate ion molecule complexes

(48) Lifshitz, C.; Elam, M.; Kababia, S., unpublished results.

(49) Potapov, V. K.; Karachevtsev, G. V.; Lipei, M. M. *Khim. Vys. Energ.* **1977**, *11*, 107.
(50) Murad, E.; Inghram, M. G. *J. Chem. Phys.* **1964**, *40*, 3263.
(51) Murad, E., Inghram, M. G. *J. Chem. Phys.* **1964**, *41*, 404.
(52) Traeger, J. C.; McLoughlin, R. G.; Nicholson, A. J. C. *J. Am. Chem. Soc.* **1982**, *104*, 5318.
(53) Potapov, V. K.; Filyngina, A. D.; Shigorin, D. N.; Ozerova, G. A. *Dokl. Akad. Nauk SSSR* **1968**, *180*, 398.
(54) Trott, W. M.; Blais, N. C.; Walters, E. A. *J. Chem. Phys.* **1978**, *69*, 3150.

has a profound effect on the kinetics and dynamics of the dissociations. This has been demonstrated here for hydrogen-bridged complexes, as well as previously[55] for ion/dipole complexes. The complexes need not reside in deep potential energy wells. The hydrogen-bridged complex treated here resides in a very shallow well. It has already been suggested previously[14,17] that transition structure switching[56,57] can lead to "entropic wells" in which the system tends to linger. A species is considered an ion/neutral complex if it exists long enough between the points at which covalent bond-breaking and the overcoming of long-range attractive forces take place so that a chemical reaction other than dissociation has time to occur.[17] In ionized acetone, dissociation leads to methyl loss, but the methyl is attracted by an ion-induced dipole attraction to the acetyl cation below its dissociation limit. It is free to move to the other methyl group within the "entropic well" and to abstract a hydrogen atom. This hydrogen abstraction reaction can only take place below its activation barrier and dominate at energies beneath the methyl dissociation limit if tunneling through a genuine barrier is allowed. Previous examples for tunneling in ionic fragmentations are scarce. The most convincing one involves tunneling through a rotational barrier in the case of the fragmentation of metastable $CH_4^{\bullet+}$ ions.[58,59]

Acknowledgment. This research was partially supported by grants from the United States–Israel Binational Science Foundation (BSF), Jerusalem. Professors M. T. Bowers and R. C. Dunbar serve as American Cooperative Investigators for these grants. F.L. thanks IAESTE for a summer fellowship. The work done at Berlin was supported by the Fonds der Chemischen Industrie, the Deutsche Forschungsgemeinschaft, and the Exchange Programme between the Technical University Berlin (T.U.B.) and the Hebrew University (H.U.) of Jerusalem. We greatly appreciate the support by the Computer Centre of T.U.B. and are grateful to Professor T. Baer and Professor J. C. Morrow for helpful comments. We are indebted to Professor D. J. McAdoo for providing us with manuscripts prior to their publication.

Registry No. $C_3H_6O^{\bullet+}$, 34484-11-2; D_2, 7782-39-0.

(55) Shao, J. D.; Baer, T.; Morrow, J. C.; Fraser-Monteiro, M. L. *J. Chem. Phys.* **1987**, *87*, 5242.
(56) Chesnavich, W. J.; Bass, L.; Su, T.; Bowers, M. T. *J. Chem. Phys.* **1981**, *74*, 2228.
(57) Bowes, M. T., Jarrold, M. F.; Wagner-Redeker, W., Kemper, P. R.; Bass, L. M. *Faraday Discuss. Chem. Soc.* **1983**, *75*, 57.
(58) Illies, A. J.; Jarrold, M. F.; Bowers, M. T. *J. Am. Chem. Soc.* **1982**, *104*, 3587.
(59) For a further discussion on tunnel effects in unimolecular dissociations of metastable ions, see ref 43a, p 236.
(60) In line with a referee's suggestion, this analysis does not necessarily fully apply to acetone ions having substantial internal energy (>21 kcal/mol). For this species, methyl loss from **2** (in particular **2a**) may by-pass the proton-bound complex **3**.

Dynamic Behavior of 1,2-Annulated Cyclooctatetraenes. Kinetic Analysis of Transition-State Steric Congestion Involving Neighboring Alicyclic Substituents

Leo A. Paquette* and Ting-Zhong Wang

Contribution from the Evans Chemical Laboratories, The Ohio State University, Columbus, Ohio 43210. *Received April 21, 1988*

Abstract: The 1,2-tetramethylene annulated cyclooctatetraene **4** has been prepared in optically active condition by three methods. When treated analogously, the 1,2-trimethylene analogue **6** has been observed to racemize too readily at room temperature and below for it to display an optical rotation. The first-order rate constants for racemization of (+)-**4** at 30.0, 40.0, and 50.0 °C were determined. When compared to the rates of bond shifting in the 1,8-tetramethylene isomer **5** (at 40–60 °C), appropriate processing of which also gives the k_{BS} rates for **4**, the rates of racemization of (+)-**4** are found to be dominated by dynamical ring inversion. Not only were the consequences of the Mills–Nixon effect quantified, but the basis for recognizing [8]annulenes as passing through planar, alternate transition states during ring inversion was further extended. The likely source of the greater conformational flexibility of **6** relative to **4** is discussed.

The long-standing preoccupation of organic chemists with the possible stabilization of one Kekulé form of a benzene derivative relative to the other was formally enunciated in 1930[1] and the stabilization has become known as the Mills–Nixon effect.[2] The suspicion at that time was that fusion of a five-membered ring to phenol as in **1** would, for geometric reasons, cause **1a**, with two of its double bonds exo to the annulated cycle, to be preferred over **1b**. Of course, no rigid fixation of double bonds is operative

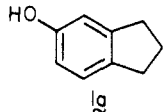

1a

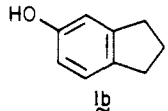

1b

in indans, nor in the lower homologous benzocyclobutenes[3] and benzocyclopropenes.[4] Several theoretical treatments of the subject have appeared,[5-8] the most compelling being due to Streitwieser and to Finnegan. They concluded that annulation can serve to

(1) Mills, W. H.; Nixon, I. G. *J. Chem. Soc.* **1930**, 2510.
(2) Fieser, L. F. In *Organic Chemistry*, 2nd ed.; Gilman, H., Ed.; Wiley: New York, 1943; Vol. I, pp 134–142.
(3) (a) Klundt, I. *Chem. Ber.* **1970**, *70*, 471. (b) Thummel, R. P. *Acc. Chem. Res.* **1980**, *13*, 70. (c) Santiago, C.; Gandour, R. W.; Houk, K. N.; Nutakul, W.; Cravey, W. E.; Thummel, R. P. *J. Am. Chem. Soc.* **1978**, *100*, 3730.
(4) (a) Halton, B. *Chem. Rev.* **1973**, *73*, 113. (b) Billups, W. E. *Acc. Chem. Res.* **1978**, *11*, 245.
(5) Longuet-Higgins, H. C.; Coulson, C. A. *Trans. Faraday Soc.* **1946**, *42*, 756.
(6) Streitwieser, A., Jr.; Ziegler, G. R.; Mowery, P. C.; Lewis, A.; Lawler, R. G. *J. Am. Chem. Soc.* **1968**, *90*, 1357.
(7) Cheung, C. S.; Cooper, M. A.; Manatt, S. L. *Tetrahedron* **1971**, *27*, 701.
(8) Finnegan, R. A. *J. Org. Chem.* **1965**, *30*, 1333.

0002-7863/88/1510-8192$01.50/0